JOURNAL OF SOLID STATE CHEMISTRY **132,** 88–97 (1997)
ARTICLE NO. SC977413

p–T Phase Diagram of $CuMoO_4$

M. Wiesmann,* H. Ehrenberg,* G. Miehe,* T. Peun,† H. Weitzel,* and H. Fuess*

*Fachgebiet Strukturforschung, Fachbereich Materialwissenschaft, Technische Hochschule Darmstadt, D-64287 Darmstadt, Federal Republic of Germany; and †Geoforschungszentrum, Telegraphenberg A17, D-14407 Potsdam, Federal Republic of Germany

Received January 29, 1997; in revised form April 2, 1997; accepted April 3, 1997

Three distinct phases of $CuMoO_4$ were observed and characterized by crystal structure analysis from single crystal and powder X-ray diffraction data. The phase stable at room temperature and ambient pressure is α-$CuMoO_4$. A phase transition from α-$CuMoO_4$ to γ-$CuMoO_4$ is observed in single crystal experiments during cooling at 190 K for ambient pressure as well as for increasing pressure at 0.2 GPa and room temperature. At temperatures above 500 K and with pressure applied both α- and γ-$CuMoO_4$ transform to $CuMoO_4$-III of distorted wolframite structure. If pressure is released after cooling, $CuMoO_4$-III remains stable to the lowest temperatures examined, but an irreversible transition from $CuMoO_4$-III to α-$CuMoO_4$ with a transition enthalpy of -15.3 kJ/mol occurs at $T = 752$ K if heated without pressure applied. In this contribution the proposed *p–T* phase diagram of $CuMoO_4$ is determined with energy dispersive synchrotron radiation from powder sample from ambient pressure up to 7.0 GPa and in the temperature range between 180 and 1293 K. The high-pressure modifications of $CuMoO_4$ are also obtained under ambient conditions, if some of the Mo ions are replaced by W. A detailed discussion of the structural relationship between α- and γ-$CuMoO_4$ is given. © 1997 Academic Press

INTRODUCTION

During the past decade the interest in the relationship between crystal structures and physical properties has experienced a revival with the discovery of high-temperature superconductivity and its severe dependence on details of the crystal structure. Namely the coordination of Cu by O and the linking of these coordination polyhedra to networks seem to be crucial points whether a compound exhibits superconductivity or not. An aspect of recent research is to study the effect of pressure on superconducting properties. Although quarternary oxides are in the center of interest, the influence of the application of pressure on the Cu coordination and connectivity schemes can better be studied in less complex systems. An enhanced understanding in this field can be a useful guide in the search for new superconducting compounds, because similar effects might be achieved by the doping or replacement with more voluminous atoms. A promising system for this purpose is $CuMoO_4$, for which up to now five different modifications have been reported in the literature (1–6). Their crystallographic data are summarized in Table 1. It depends on pressure and temperature as well as on the conditions of synthesis which of these modifications is formed. At ambient pressure and room temperature α-$CuMoO_4$ (1) is the stable modification, while for temperatures above 840 K a high-temperature modification of hexagonal symmetry, β-$CuMoO_4$, has been reported, but neither its space group nor its atomic parameters are given (2, 3). From high-pressure syntheses two modifications, $CuMoO_4$-II (4) and $CuMoO_4$-III (5), were described, which remain stable at ambient pressure and to low temperatures. For both types triclinic distorted wolframite structures are assumed, but atomic parameters are determined only for $CuMoO_4$-III. Furthermore the γ-modification, which is stable below 190 K and ambient pressure, has recently been reported (6).

The four modifications α-, γ-, -II, and -III under consideration differ in their Cu and Mo coordination. In α-$CuMoO_4$ the three molybdenum atoms are tetrahedrally coordinated by oxygen and, using the labeling of Table 2, the Cu(1) and Cu(2) atoms are octahedrally surrounded, while Cu(3) atoms are square-pyramidally surrounded. These polyhedra are interconnected via common corners and edges-forming channels. In γ-$CuMoO_4$ and $CuMoO_4$-III, copper and molybdenum atoms are all octahedrally coordinated. γ-$CuMoO_4$ can be derived from a cubic close packing of oxygen atoms (6), while the distorted wolframite structure of $CuMoO_4$-III can be deduced from a hexagonal close packing with atomic parameters very similar to those of $CuWO_4$. The X-ray powder lines observed for $CuMoO_4$-II have been indexed by Sleight based on a unit cell metric very similar to $CuWO_4$, but no structural parameters were derived (4). Chemical pressure can be achieved by replacing some of the Mo ions by W. The influence of inner pressure on the stability ranges was investigated by crystal structure determination of mixed compounds $Cu(Mo,W)O_4$.

In the present paper a *p–T* phase diagram of $CuMoO_4$ is proposed. Furthermore, an interpretation of the observed phase transitions and structural relationships, especially between α- and γ-$CuMoO_4$, is given.

0022-4596/97 $25.00

TABLE 1
The Five Different Modifications of $CuMoO_4$ as Reported in the Literature

Modification	a (Å)	b (Å)	c (Å)	α (°)	β (°)	γ (°)	Ref.
α-$CuMoO_4$	9.901(3)	6.786(2)	8.369(3)	101.13(1)	96.88(1)	107.01(1)	(1)
γ-$CuMoO_4$	9.699(9)	6.299(6)	7.966(7)	94.62(4)	103.36(4)	103.17(4)	(6)
$CuMoO_4$-II	4.6788	5.8042	4.9149	91.08	91.70	84.90	(4)
$CuMoO_4$-III	4.7366(4)	5.8637(8)	4.8720(4)	91.03(1)	92.55(1)	80.98(1)	(5)
β-$CuMoO_4$	16.079	16.079	6.723	90	90	120	(2, 3)

Note. All phases crystallize in space group $P\bar{1}$ except β-$CuMoO_4$, for which hexagonal symmetry is claimed, but neither a specific space group nor atomic parameters are given.

EXPERIMENTAL DETAILS AND RESULTS

a. Single Crystal X-Ray Diffraction

The synthesis of single crystals of α-$CuMoO_4$ is described elsewhere (1, 6). Single crystals with well-developed faces were selected and mounted in a high-pressure cell of the Merrill–Bassett type (7). A steel gasket (Inconel 715) with a hole of 400 μm obtained by spark erosion (8) was applied. A detailed description of this modified cell is reported elsewhere (9). The pressure medium was a 4:1 mixture of methanol–ethanol, and pressure was determined using the ruby fluorescence method (10). The details of high-pressure single crystal X-ray data collection and structure refinement are summarized in Table 3.

The geometric restrictions of the Merrill–Bassett high-pressure cell allow one only to record a reduced number of reflections. In all experiments the plate-like crystals were found to be oriented with their crystallographic [001] directions perpendicular to the diamond face, and therefore reflections (00l) with $l \neq 1$ could not be measured.

The refined lattice parameters are very close to those of the low-temperature modification, for which a complete data set is available, and a structure determination had been performed at 190 K (6). The similarity of both lattice constants and space group gave strong evidence that the modification at 0.2 GPa and room temperature is γ-$CuMoO_4$. A structure refinement with the atomic positions of the low-temperature structure (γ) as start parameters confirmed this assumption and led to the atomic parameters as summarized in Table 2. Only isotropic displacement factors could be refined for all atoms as a consequence of the incomplete data set. After releasing pressure γ-$CuMoO_4$ remained metastable at room temperature for about 1 h to 1 day, before the retransformation to the α-modification took place.

Mixed compounds $Cu(Mo,W)O_4$ have been synthesized under the same conditions as α-$CuMoO_4$, but with different molar ratios of the reactants CuO (99.99%, Aldrich), MoO_3 (99.5+%, Aldrich), and WO_3 (99+%, Aldrich). The Mo:W ratio was varied from 0.05 to 0.9, and two compositions are discussed in detail as representatives: Single crystals were isolated from the reaction products obtained from mixtures of CuO, MoO_3, and WO_3 in the ratios 1:0.85:0.15 and 1:0.25:0.75, respectively. Structure determinations under ambient conditions reveal the crystal structures of γ-$CuMoO_4$ for $Cu(Mo_{0.85}W_{0.15})O_4$ and of $CuMoO_4$-III for $Cu(Mo_{0.25}W_{0.75})O_4$. Details of experimental conditions and results are summarized in Tables 4–7. The substitution of Mo by W induces chemical pressure, and under the same conditions of synthesis as for the preparation of α-$CuMoO_4$ the high-pressure modifications are formed instead.

b. Powder X-Ray Diffraction

Powder experiments were performed using the multianvil high-pressure cell MAX80 at the synchrotron laboratory HASYLAB, beamline *F*2/1 (14). For this purpose a boron–nitride tube was inserted in a cylinder of graphite and both placed in a drilled boron-epoxy resin cube. A thermocouple was attached to the center of the as-prepared sample holder. Powder samples which at first were grounded in an agate mortar under acetone were filled in the boron–nitride tube. Sodium chloride, separated from the sample by a boron–nitride layer, was used for pressure calibration. The sample holder was closed by two pyrophyllite plugs, which are embraced by two copper rings to allow heating by electric current. For the experiments at room temperature α-$CuMoO_4$ was mixed with petroleum jelly in the ratio 1:3 to homogenize the pressure distribution. Energy dispersive X-ray diffractograms in the energy range from 10 to 70 keV were measured for pressures from 0.02 to 7.0 GPa in 0.5 to 1.0 GPa steps and at temperatures between 298 and 1298 K in steps of 20 to 50 K. The diffraction angle was calibrated for each run using the internal NaCl standard without pressure applied, revealing values of Θ between 2.821° and 3.239°. Diffraction peaks were fitted by Gauss profiles; the resulting d-spacings were indexed and lattice constants were refined using the program *Unitcell* (15). The powder experiments reveal three different solid phases: α-$CuMoO_4$, γ-$CuMoO_4$, and $CuMoO_4$-III with stability relations as shown in Fig. 1. Phase lines in the diagram are drawn where the predominant fraction of sample has changed between

TABLE 2
The One-to-One Correspondence between Atomic Sites in α- and γ-$CuMoO_4$

Space group		*a* (Å)	*b* (Å)	*c* (Å)
$P\bar{1}$		9.901(3)	6.786(2)	8.369(3)
$P\bar{1}$		*9.708(3)*	*6.302(7)*	*7.977(2)*
		α (°)	β (°)	γ (°)
$V_{uc}/Z = 86.37$ Å^3, $Z = 6$		101.13(1)	96.88(1)	107.01(1)
$V_{uc}/Z = 76.08$ *Å*^{3}, $Z = 6$		*94.76(2)*	*103.35(3)*	*103.26(1)*
Atom	*x*	*y*	*z*	u_{eff} (Å^2)
Mo(1)	0.3450(1)	0.1970(1)	0.0850(1)	0.009(1)
Mo(1)	*0.3481(2)*	*0.2162(2)*	*0.1267(1)*	*0.0037(1)*
Mo(2)	0.1064(1)	0.4960(1)	0.7776(1)	0.010(1)
Mo(2)	*0.1094(1)*	*0.4147(2)*	*0.8799(1)*	*0.0029(3)*
Mo(3)	0.2500(1)	0.9927(1)	0.4648(1)	0.011(1)
Mo(3)	*0.2267(1)*	*0.9336(2)*	*0.4583(1)*	*0.0033(3)*
Cu(1)	0.4054(1)	0.7466(1)	0.1983(1)	0.012(1)
Cu(1)	*0.4342(2)*	*0.7160(3)*	*0.2361(3)*	*0.0075(4)*
Cu(2)	0.9922(1)	0.0472(1)	0.2024(1)	0.011(1)
Cu(2)	*0.0069(2)*	*0.0931(3)*	*0.1938(2)*	*0.0077(4)*
Cu(3)	0.2365(1)	0.4626(1)	0.3853(1)	0.012(1)
Cu(3)	*0.3353(2)*	*0.4244(3)*	*0.5261(2)*	*0.0072(5)*
O(1)	0.1422(5)	0.9349(7)	0.6048(5)	0.026(1)
O(1)	*0.1192(12)*	*0.8962(18)*	*0.6001(15)*	*0.009(2)*
O(2)	0.2764(4)	0.7463(6)	0.3597(5)	0.014(1)
O(2)	*0.2964(11)*	*0.6986(16)*	*0.4560(14)*	*0.009(2)*
O(3)	0.1852(4)	0.1575(6)	0.3418(5)	0.014(1)
O(3)	*0.2002(12)*	*0.2090(18)*	*0.3454(14)*	*0.010(2)*
O(4)	0.1649(4)	0.0652(7)	0.9866(5)	0.018(1)
O(4)	*0.1546(12)*	*0.1263(17)*	*0.9699(14)*	*0.009(2)*
O(5)	0.1838(6)	0.5017(7)	0.5985(5)	0.025(1)
O(5)	*0.1931(12)*	*0.4488(19)*	*0.7160(14)*	*0.017(2)*
O(6)	0.3664(4)	0.4507(6)	0.2229(5)	0.013(1)
O(6)	*0.4753(12)*	*0.4359(19)*	*0.2991(14)*	*0.013(2)*
O(7)	0.2404(5)	0.5941(9)	0.9499(6)	0.027(1)
O(7)	*0.2720(11)*	*0.5024(17)*	*0.0747(14)*	*0.010(2)*
O(8)	0.4132(5)	0.1566(7)	0.5765(6)	0.025(1)
O(8)	*0.3866(12)*	*0.1492(16)*	*0.5881(14)*	*0.012(2)*
O(9)	0.0047(5)	0.2308(7)	0.7699(6)	0.021(1)
O(9)	*0.9401(11)*	*0.1825(16)*	*0.7561(13)*	*0.009(2)*
O(10)	0.0109(4)	0.3464(6)	0.2116(5)	0.016(1)
O(10)	*0.9737(12)*	*0.3612(17)*	*0.1092(14)*	*0.010(2)*
O(11)	0.4470(5)	0.2508(7)	0.9351(5)	0.021(1)
O(11)	*0.4473(12)*	*0.2089(19)*	*0.9783(14)*	*0.018(2)*
O(12)	0.4104(4)	0.0354(7)	0.1923(6)	0.017(1)
O(12)	*0.3568(11)*	*0.9728(17)*	*0.2219(14)*	*0.009(2)*

Note. Atomic parameters at room temperature for α-$CuMoO_4$ at ambient pressure (6) and for γ-$CuMoO_4$ at 0.2 GPa (*italic*) as derived from single crystal X-ray diffraction.

both phases for pathes either at constant temperature and increasing pressure or at constant pressure and increasing temperature. These lines do not neccessarily represent an equilibrium and therefore are called probable phase lines. The possible periods for examinations under fixed conditions of temperature and pressure are restricted to a few minutes, so that the constancy of phase properties with the passage of time cannot be used as criterion for equilibrium in this system. More informative is the comparison of properties at the same conditions, with respect to the variants, but reached from different directions or by different procedures. This criterion confirms the stability of $CuMoO_4$-III in the region shown in Fig. 1, because this phase can be obtained from γ-$CuMoO_4$ either by heating or by applying pressure to α-$CuMoO_4$. In contrast the stability range of γ-$CuMoO_4$ is questionable, because this phase can be obtained at room temperature only by applying pressure to α-$CuMoO_4$, but not by cooling from $CuMoO_4$-III. No retransformation from $CuMoO_4$-III was observed, if pressure is released after cooling. On the other hand, a phase transition to α-$CuMoO_4$ takes place, if pressure is released at high-temperature. No reflections of another high-pressure modification of $CuMoO_4$-II nor of the proposed high-temperature phase β-$CuMoO_4$ have been observed.

The inverse compressibility, i.e., the bulk modulus $K(p)$, can be expanded in a power series in pressure p:

$$K(p) = K_0 + K_0' p + \cdots,$$

$$K_0 = K(p = 0), \qquad [1]$$

$$K_0' = \left(\frac{\partial K}{\partial p}\right)_T \quad (p = 0).$$

The parameters K_0 and K_0' can be derived by fitting the equation of state

$$P = \frac{K_0}{K_0'}\left[\left(\frac{V_0}{V}\right)^{K_0'} - 1\right], \qquad [2]$$

published by Murnaghan (16) to the observed pressure versus volume data. The empirical Eq. [2] is appropriate for compressions $(V_0 - V)/V \leq 0.15$ with V_0 as volume at $p = 0$.

For the α-modification at room temperature the coefficient $K_0 = 59.4(3.5)$ GPa was obtained using data up to 0.7 GPa. As a consequence of this small pressure range K_0' was kept fixed to a typical value of 4.4. A two phase region between 0.7 and 1.1 GPa follows, where α- and γ-$CuMoO_4$ coexist. From data at higher pressures the parameters $K_0 = 44.0(3.4)$ GPa and $K_0' = 15.3(3.0)$ are derived for γ-$CuMoO_4$ at room temperature, where the volume at zero pressure, $V_0 = 466(2)$ Å^3 must be extrapolated. The

TABLE 3
Details of X-Ray Single Crystal Data Collection and Structure Refinement for the Experiment at 0.20(3) GPa and Room Temperature

Diffractometer: ENRAF NONIUS CAD4	Radiation: Mo$K\alpha$, $\lambda = 0.71093$ Å
Fine-focus sealed tube	Graphite monochromator
Detector: scintillation counter	Pulse-height-discrimination
ω-scan	Cell parameters from 25 reflections ($10.49^\circ \le 2\theta \le 42.22^\circ$)
Crystal size: $0.10 \times 0.18 \times 0.04$ mm	Crystal habit: plate
Crystal color: red	
$h = -8 \to 8$	1499 measured reflections ($4.46^\circ \le 2\theta \le 59.62^\circ$)
$k = -9 \to 9$	781 independent reflections [R(int) = 0.0420]
$l = -13 \to 13$	Linear absorption coefficient: 10.38 mm^{-1}
Absorption correction: empiric	Finger and King (11)
Refinement method (74 parameters):	Full-matrix least-squares on F^2
Goodness of fit: $S = 1.107$	$\Delta\rho_{max} = 5.008\ e\ Å^{-3}$, $\Delta\rho_{min} = -4.260\ e\ Å^{-3}$
Final R indices [$I > 2\sigma(I)$]:	$R_1 = 0.1097$, $wR_2 = 0.3279$
R indices (all data):	$R_1 = 0.1107$, $wR_2 = 0.3282$
Atomic scattering factors from:	Int. Tables Vol. IV, Tables 2.2B and 2.3.1
Structure refinement: SHELXS-86 (12), SHELXL-93 (13)	

given uncertainties are derived for a criterion of a 10% higher deviation between calculated and observed data as compared with the best fit. The dependence of V/V_0 on pressure and the best fits according to the Murnaghan Equation of State [2] are presented in Fig. 2, where the coexistence range of both phases α and γ has been excluded. In Fig. 3 cell parameters at room temperature versus pressure are shown.

Additional X-ray powder experiments in the temperature range from 130 to 970 K at ambient pressure were performed with Cu$K\alpha_1$ radiation in Debye–Scherrer geometry. Intensity data were collected in the range of $10^\circ \le 2\Theta \le 60^\circ$ with a position-sensitive detector (6° aperture) and have been analyzed by the Rietveld method (17). In Fig. 4 the temperature dependence of the refined cell constants of α-$CuMoO_4$ is presented for temperatures between 273 and 973 K. From the change of volume with temperature a linear thermal expansion coefficient $\alpha_T = 6.2(1) \times 10^{-6}\ K^{-1}$ can be obtained for α-$CuMoO_4$.

At ambient pressure a transformation from $CuMoO_4$-III to α-$CuMoO_4$ takes place during heating at $T = 752$ K with a transition enthalpy of -15.3 kJ/mol. This phase transition was studied by both X-ray powder diffraction and DSC. An analogous transition is reported for $CuMoO_4$-II

TABLE 4
Details of X-Ray Single Crystal Data Collection and Structure Refinement for $Cu(Mo_{0.85}W_{0.15})O_4$

Diffractometer: ENRAF NONIUS CAD4	Radiation: Mo$K\alpha$, $\lambda = 0.71093$ Å
Fine-focus sealed tube	Graphite monochromator
Detector: scintillation counter	Pulse-height-discrimination
θ 2θ-scan	Cell parameters from 25 reflections ($5.9^\circ \le 2\theta \le 36.5^\circ$)
Crystal size: $0.10 \times 0.05 \times 0.025$ mm	Crystal habit: orthorhombic prism
Crystal color: red	
$h = -15 \to 15$	5947 measured reflections ($7.71^\circ \le 2\theta \le 60.41^\circ$)
$k = -10 \to 10$	4011 independent reflections [R(int) = 0.1301]
$l = -12 \to 4$	Linear absorption coefficient: 15.8 mm^{-1}
Absorption correction: empiric	Transmission: $0.239 \le T \le 0.536$
Refinement method (167 parameters)	Full-matrix least-squares on F^2
Goodness of fit: $S = 0.981$	$\Delta\rho_{max} = 4.084\ e\ Å^{-3}$, $\Delta\rho_{min} = -5.796\ e\ Å^{-3}$
Final R indices ($I > 2\sigma(I)$)	$R_1 = 0.0471$, $wR_2 = 0.1115$
R indices (all data)	$R_1 = 0.0977$, $wR_2 = 0.1378$
Extinction correction: empiric	$\left[1 + \frac{xF_c^2\lambda^3}{1000\sin(2\Theta)}\right]^{-\frac{1}{4}}$, $x = 0.062(4)$
Atomic scattering factors from	Int. Tables Vol. IV, Tables 2.2B and 2.3.1
Structure refinement: SHELXS-86 (12), SHELXL-93 (13)	

TABLE 5
Atomic Parameters for $Cu(Mo_{0.85}W_{0.15})O_4$ at Room Temperature as Derived from X-Ray Single Crystal Diffraction

			a (Å)	b (Å)	c (Å)
Space group			9.713(1)	6.305(1)	7.977(1)
$P\bar{1}$			α (°)	β (°)	γ (°)
$V_{uc}/Z = 76.32$ Å^3, $Z = 6$			94.70(2)	103.31(1)	103.30(1)
Atom	x	y	z	u_{eff} (Å^2)	Occupancy
Mo/W(1)	0.3476(1)	0.2169(1)	0.1272(1)	0.009(1)	0.80/0.20(1)
Mo/W(2)	0.1089(1)	0.4136(1)	0.8803(1)	0.009(1)	0.84/0.16(1)
Mo/W(3)	0.2272(1)	0.9339(1)	0.4584(1)	0.010(1)	0.91/0.09(1)
Cu(1)	0.4346(1)	0.7835(2)	0.2351(1)	0.012(1)	1
Cu(2)	0.0066(1)	0.0935(2)	0.1946(1)	0.011(1)	1
Cu(3)	0.3350(1)	0.4241(1)	0.5263(1)	0.011(1)	1
O(1)	0.1194(6)	0.3973(10)	0.5994(7)	0.018(1)	1
O(2)	0.2956(7)	0.1970(9)	0.4546(7)	0.015(1)	1
O(3)	0.1997(6)	0.7082(9)	0.3405(6)	0.012(1)	1
O(4)	0.1533(6)	0.1243(8)	0.9702(8)	0.012(1)	1
O(5)	0.1928(7)	0.4521(10)	0.7160(8)	0.021(1)	1
O(6)	0.4766(6)	0.4360(9)	0.3014(7)	0.013(1)	1
O(7)	0.2722(6)	0.5034(10)	0.0752(7)	0.017(1)	1
O(8)	0.3868(6)	0.6490(9)	0.5893(7)	0.015(1)	1
O(9)	0.9412(7)	0.1851(9)	0.7585(7)	0.014(1)	1
O(10)	0.9739(6)	0.3611(9)	0.1077(7)	0.014(1)	1
O(11)	0.4486(7)	0.2104(11)	0.9798(7)	0.012(1)	1
O(12)	0.3571(6)	0.5272(11)	0.2214(7)	0.015(1)	1

The amount of W, averaged over all sites, was confirmed by EDX to be 15(1)%.

(4). Raman studies on $CuMoO_4$-III were not successful because of a transition to α-$CuMoO_4$ induced by local heating due to radiation absorption effects.

TABLE 7
Atomic Parameters for $Cu(Mo_{0.25}W_{0.75})O_4$ at Room Temperature as Derived from X-Ray Single Crystal Diffraction

			a (Å)	b (Å)	c (Å)
Space group			4.714(2)	5.848(2)	4.879(2)
$P\bar{1}$			α (°)	β (°)	γ (°)
$V_{uc}/Z = 66.56$ Å^3, $Z = 2$			91.51(2)	92.48(2)	82.35(2)
Atom	x	y	z	u_{eff} (Å^2)	Occupancy
Mo/W	0.0244(1)	0.1735(1)	0.2452(1)	0.008(1)	0.24(1) /0.76(1)
Cu	0.4940(2)	0.6588(1)	0.2554(1)	0.011(1)	1
O(1)	0.2502(10)	0.3534(9)	0.4263(9)	0.012(1)	1
O(2)	0.2145(9)	0.8792(8)	0.4281(8)	0.010(1)	1
O(3)	0.7344(10)	0.3806(8)	0.0984(9)	0.011(1)	1
O(4)	0.7829(10)	0.9076(8)	0.0518(8)	0.011(1)	1

The existence of the proposed high-temperature modification β-$CuMoO_4$ (2, 3) was not confirmed, neither in high-temperature X-ray experiments up to 973 K nor in calorimetric investigations.

DISCUSSION

The phase transition between α-$CuMoO_4$ and γ-$CuMoO_4$ (see Table 2 for atomic parameters) at temperatures between 180 and 200 K and ambient pressure is also observed at room temperature and a pressure of 0.20(3) GPa in a single crystal experiment. This phase transition is of first order involving a volume reduction of 12–13%. Similar to the behavior at low-temperature at ambient pressure a pronounced hysteresis effect is observed:

TABLE 6
Details of X-Ray Single Crystal Data Collection and Structure Refinement for $Cu(Mo_{0.25}W_{0.75})O_4$

Diffractometer: STOE STADI 4	Radiation: Mo$K\alpha$, $\lambda = 0.71093$ Å
Fine-focus sealed tube	Graphite monochromator
Detector: scintillation counter	Pulse-height-discrimination
θ 2θ-scan	Cell parameters from 48 reflections ($14.08° \le 2\theta \le 79.84°$)
Crystal size: $0.05 \times 0.08 \times 0.1$ mm	Crystal habit: orthorhombic prism
Crystal color: black	
$h = -7 \to 7$	2352 measured reflections ($7.04° \le 2\theta \le 69.92°$)
$k = -7 \to 7$	1176 independent reflections [R(int) = 0.0729]
$l = -9 \to 9$	Linear absorption coefficient: 41.32 mm^{-1}
Absorption correction: empiric	Transmission: $0.0377 \le T \le 0.0852$
Refinement method (57 parameters):	Full-matrix least-squares on F^2
Goodness of fit: $S = 1.097$	$\Delta\rho_{max} = 4.346\ e$ Å^{-3}, $\Delta\rho_{min} = -4.813\ e$ Å^{-3}
Final R indices [$I > 2\ \sigma(I)$]:	$R_1 = 0.0343$, $wR_2 = 0.0820$
R indices (all data):	$R_1 = 0.0364$, $wR_2 = 0.0831$
Extinction correction: empiric	$\left[1 + \frac{xF_c^2\lambda^3}{1000\sin(2\Theta)}\right]^{-\frac{1}{4}}$, $x = 0.0009(6)$
Atomic scattering factors from:	Int. Tables Vol. IV, Tables 2.2B and 2.3.1
Structure refinement: SHELXS-86 (12), SHELXL-93 (13)	

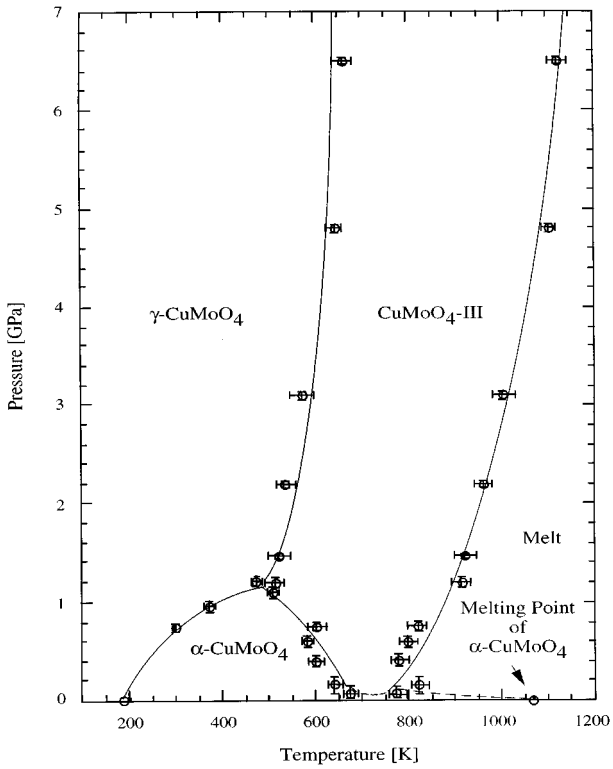

FIG. 1. p–T phase diagram of $CuMoO_4$. Between 670 and 770 K the required pressure for the stabilization of $CuMoO_4$-III instead of α-$CuMoO_4$ was within pressure resolution of the instrument, and therefore the phase boundary could not be determined. The dashed line is shown to emphasize that α-$CuMoO_4$ is stable in this temperature region if no pressure is applied.

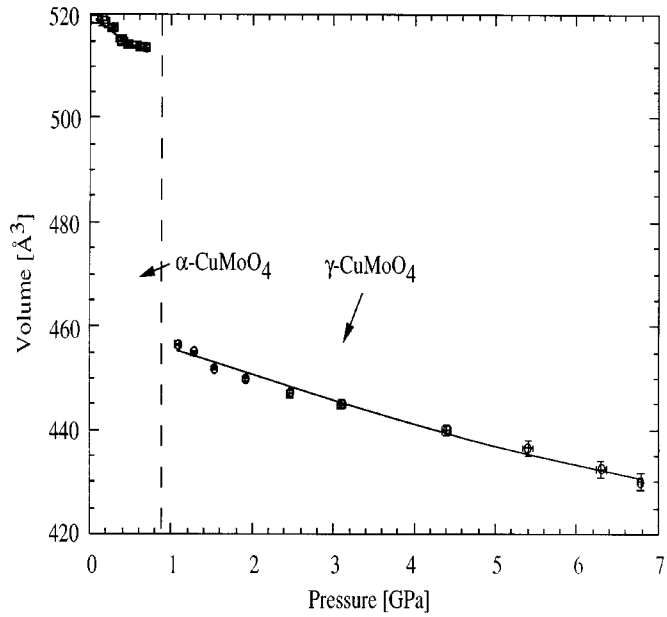

FIG. 2. Volume vs pressure at room temperature fitted to the Murnaghan Equation of State [2].

After releasing pressure γ-$CuMoO_4$ remains metastable at ambient pressure but a transition to the α-modification can be induced by heating. During this phase transition $\gamma \rightarrow \alpha$ the coordination of the two copper atoms Cu(1) and Cu(2) remains almost unchanged, while the coordination of Cu(3) changes from octahedral to tetragonal pyramidal. The molybdenum atoms, distorted octahedrally coordinated in the γ-modification, become tetrahedrally coordinated in the α-modification. This phase transition is *pseudoreconstructive*: On the one hand bonds are broken and the topology is changed, and on the other hand no diffusion of atoms takes place.

As pointed out previously (6) the γ-modification can be considered as a defective NaCl-type structure. Only $\frac{4}{9}$ of the cation sites and $\frac{8}{9}$ of the anion sites are occupied. The matrix M_1,

$$M_1 = \begin{pmatrix} \frac{7}{27} & \frac{1}{27} & -\frac{11}{27} \\ \frac{1}{3} & \frac{1}{3} & \frac{1}{3} \\ \frac{1}{9} & -\frac{5}{9} & \frac{1}{9} \end{pmatrix}, \quad \det(M_1) = \frac{4}{27}, \qquad [3]$$

transforms the γ-$CuMoO_4$ cell to the NaCl cell. Hence the directions [7 1 −11], [1 1 1] and [1 −5 1] are prominent in γ-$CuMoO_4$: The "channels" (cf. (6)) run along [1 1 1]; the "layers" are spanned by the vectors [1 1 1] and [1 −5 1] and are stacked in the direction [7 1 −11], i.e., the viewing direction in Fig. 5. A pseudo mirror plane is spanned by the vectors [−1 −1 2] and [−1 1 1] or, equivalent, in terms of the prominent directions by [7 1 −11] and [1 −5 1]. Together with pseudo 2- and 2_1-axes parallel [1 1 1] this mirror plane belongs to the set of symmetry elements of space group $A12/m1$, by which a hypothetic structure very close to the γ-$CuMoO_4$ structure can be described. The pseudo symmetries are clearly visible in Fig. 5a. They partially transform Cu into Mo atoms and vice versa and are made possible by the similar octahedral coordination of both atomic species. The matrix M_2,

$$M_2 = \begin{pmatrix} \frac{1}{3} & \frac{1}{3} & -\frac{2}{3} \\ \frac{1}{3} & \frac{1}{3} & \frac{1}{3} \\ \frac{1}{3} & -\frac{5}{3} & \frac{1}{3} \end{pmatrix}, \quad \det(M_2) = \frac{2}{3}, \qquad [4]$$

transforms the γ-$CuMoO_4$ cell to this "pseudomonoclinic" A-centered cell with $a = 7.060$ Å, $b = 3.733$ Å, $c = 12.005$ Å, $\alpha = 90.52°$, $\beta = 105.47°$, and $\gamma = 89.84°$ as realized in $AlNbO_4$ (6). In reciprocal space the pseudo-subcell becomes apparent in the stronger average intensities of reflections belonging to the parity group $h + k + l = 3n$.

The change from octahedral to tetrahedral coordination for the Mo atoms destroys the pseudosymmetries. The correspondence of the atoms in both structures, however, is

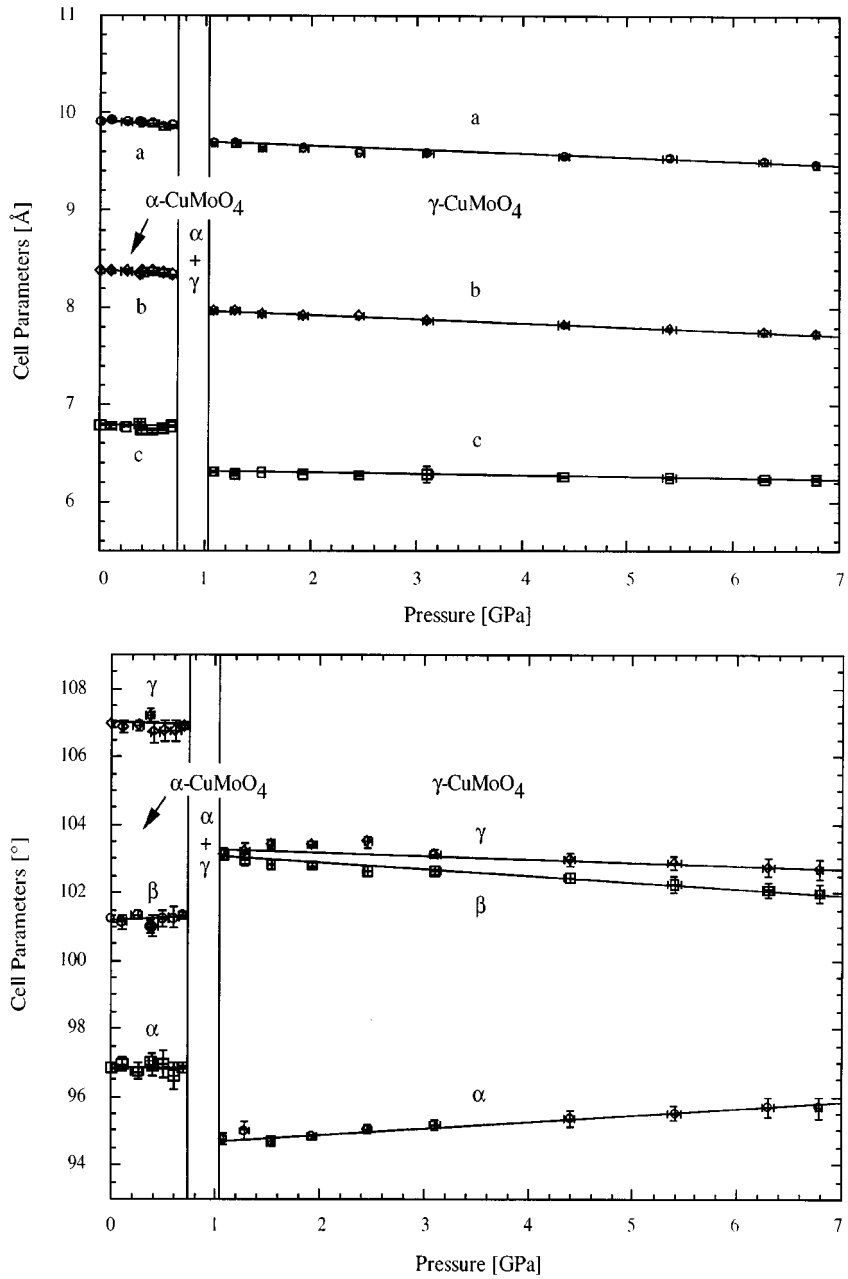

FIG. 3. Cell parameters vs pressure at room temperature.

unique (cf. Table 2), and the connectivities are partially preserved. In particular, the layer-like character of the structure is still present in the α-modification. Again the layers are stacked in the [7 1 −11] direction and the linkage is imparted by the same oxygen atoms as in the γ-modification.

The changes within a layer are drastic and sketched in Fig. 5. To visualize the degree of distortion during this phase transition, in Fig. 5a one layer of the γ-phase is projected down [7 1 −11]. The black dots indicate the subset of inversion centers which acts within the layer. A nearly quadratic array of 8×8 fields (corresponding to 4×4 NaCl cells) is contoured by bold lines, and the fields are stippled alternating in the way of a chess board. Figure 5b shows how this chess board is deformed. Only bonds closer than 2.7 Å are drawn; the nonbonded oxygens outside the array in Fig. 5b had been bonded in Fig. 5a. The structure of α-$CuMoO_4$ is presented in Fig. 6. The Cu(3) atom is coordinated by five oxygen atoms, building a distorted tetrahedral pyramid.

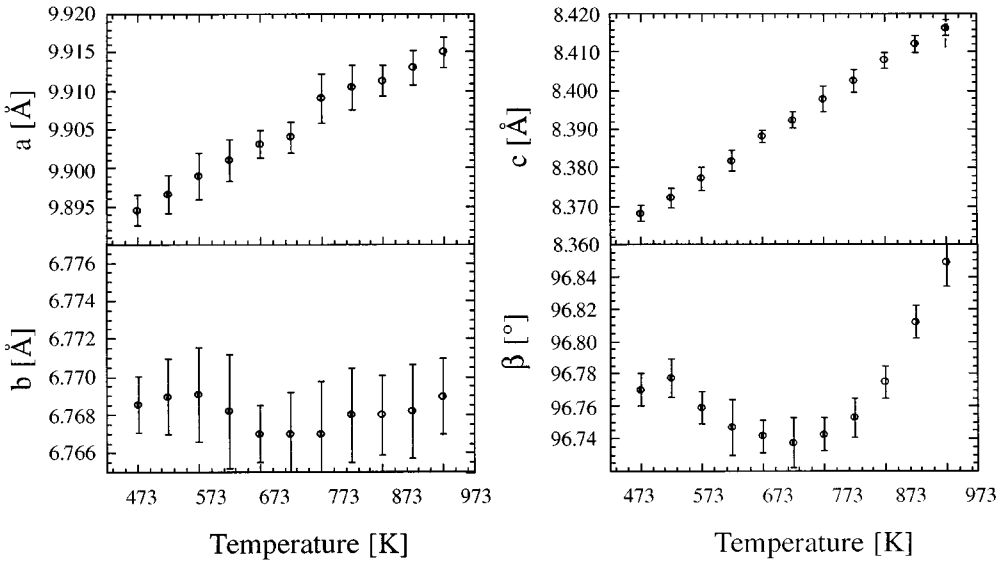

FIG. 4. Cell parameters vs temperature for α-$CuMoO_4$ at ambient pressure. For the angles α and γ no pronounced temperature dependence was observed.

Visually the phase transition $\alpha \rightarrow \gamma$ is accompanied by a change in color from light green to red. As expected for a first-order phase transition both phases are separated by a two-phase region. As seen in Fig. 1 the phase transition between α- and γ-modification takes place at temperatures between 190 K and about 480 K, transition temperature increasing with pressure applied. A first-order phase transition to $CuMoO_4$-III takes place from both the α- and the γ-modification, but no ranges of coexistence have been observed here. Both high-pressure modifications (γ- and -III) return to α-$CuMoO_4$ when pressure is released and temperature increased. A triple point is detected in the pressure range between 1.1 and 1.2 GPa and a temperature between 460 and 530 K. The phase transition $\alpha \rightarrow$ III can be observed down to the lowest significant pressure applied of 0.15(10) GPa, but in high-temperature X-ray experiments at ambient pressure no phase transition to $CuMoO_4$-III had been detected. This fact leads to the conclusion that there

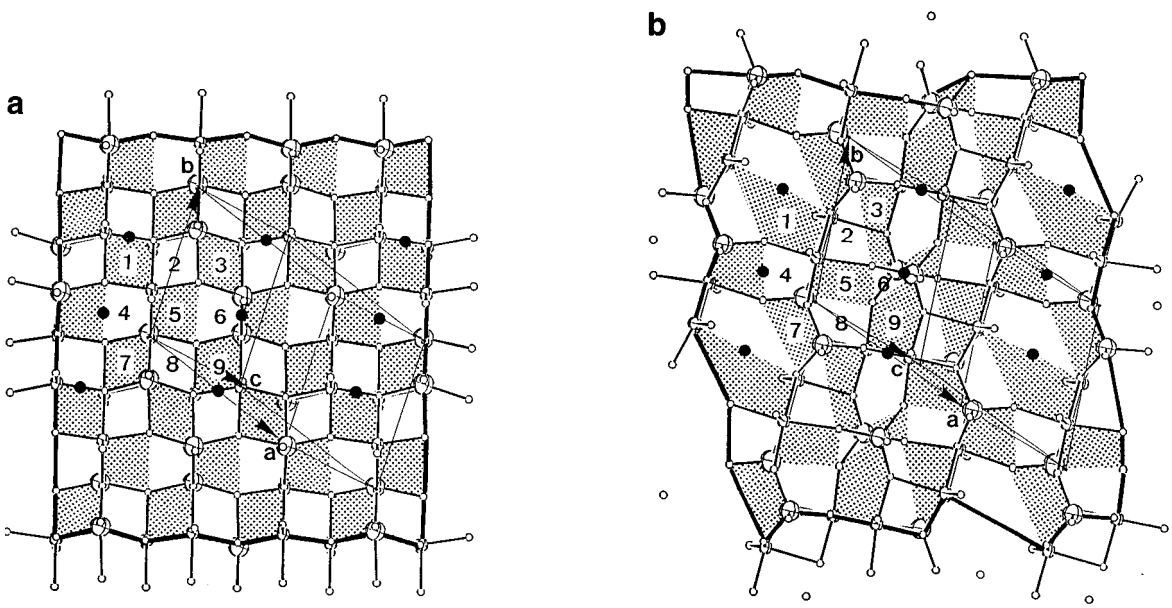

FIG. 5. Projection of a single layer down [7 1 −11] for (a) γ-$CuMoO_4$ and (b) α-$CuMoO_4$. The atomic spheres are big, Mo; medium, Cu; and small, O. Both projections are drawn to exactly the same scale.

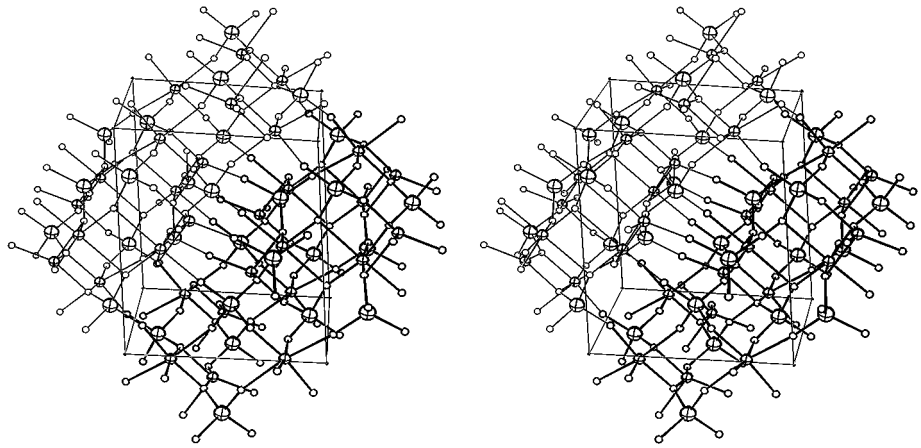

FIG. 6. Stereo pair of α-$CuMoO_4$. Two layers are shown; one of them is accentuated by bold lines. **a** points up; **c** points right. The assignment of atoms is as in Fig. 5.

has to be a phase boundary between $CuMoO_4$-III and α-$CuMoO_4$ in the temperature range between 673 and 773 K at pressures lower than 0.1 GPa. A precise determination of applied pressure in the range from 0 to 0.1 GPa was not possible with the used instrumental setup. The pressure dependence of melting temperature was not resolved below 0.1 GPa. In Fig. 1 a linear interpolation between the melting points at ambient pressure and 0.1 GPa is shown as a dashed line.

The structure of $CuMoO_4$-III (5) is a triclinic distorted wolframite structure similar to that of $CuWO_4$, where Cu and Mo atoms are octahedrally coordinated by oxygen atoms (18). The notation -III is rather misleading, since the high-pressure modifications of the other transition metal molybdates, Me = Fe, Co, and Ni, are labeled $Me$$MoO_4$-II (19). These modifications are also of wolframite structure and formed under similar conditions with either α-modifications or MeO and MoO_3 as reactants. The notation $CuMoO_4$-II was previously used by Sleight (4) for another modification obtained by high-pressure synthesis from the oxides CuO and MoO_3 at 5.8 GPa and 950°C in a gold container. The conditions are different for our procedure: By heating and applying pressure to previously synthesized α-$CuMoO_4$ we always obtained $CuMoO_4$-III. Based on the similarity of lattice constants derived from powder patterns, Sleight has drawn the conclusion that his modification $CuMoO_4$-II should be isostructural to $CuWO_4$, but no atomic parameters are given. If we use the settings of Table 1 and the atomic parameters of $CuWO_4$ (18) or $CuMoO_4$-III (5), both determined from single crystal X-ray data, and calculate a powder diagram with the lattice constants of $CuMoO_4$-II, these calculated intensities for $CuMoO_4$-II are not in satisfactory agreement with the observed ones published by Sleight (4). Therefore, the atomic parameters must be different in both high-pressure modifications -II and -III, if the same setting is used; in other words, both structure types represent different kinds of triclinic distortions of the monoclinic wolframite structure, although it is possible to set up the unit cell of $CuMoO_4$-II ($V_{uc}/Z = 66.44$ Å^3) in such a way that very similar lattice constants for $CuMoO_4$-II on the one hand and $CuMoO_4$-III ($V_{uc}/Z = 66.75$ Å^3) and $CuWO_4$ ($V_{uc}/Z = 66.37$ Å^3) on the other hand result. For $CuMoO_4$-II a phase transition to the α-modification is reported between 673 and 773 K. If $CuMoO_4$-II is really another high-pressure modification, its thermal stability is therefore similar to that of $CuMoO_4$-III, where we observed the analogous transition at 752 K.

ACKNOWLEDGMENTS

Support by the Deutsche Forschungsgemeinschaft (Grant We 1542/3-1) and by the Fond der Chemischen Industrie is gratefully acknowledged. This work has further benefitted from allocated beam time at HASYLAB, Germany. Also the supply of the Merrill–Bassett high-pressure cell and the introduction of high pressure techniques by H. Ahsbahs, University of Marburg, Germany, is gratefully acknowledged.

REFERENCES

1. S. C. Abrahams, J. L. Bernstein, and P. B. Jamieson, *J. Chem. Phys.* **48**, 2619 (1968).
2. R. Kohlmuller and J.-P. Faurie, *C. R. Acad. Sci.* **264C,** 1751 (1967).
3. R. Kohlmuller and J.-P. Faurie, *Bull. Soc. Chim. Fr.* 4379 (1968).
4. A. W. Sleight, *Mater. Res. Bull.* **8,** 863 (1973).
5. R. Tali, V. V. Tabachenko, L. M. Kovba, L. N. Dem'yanets, *Russ. J. I. Chem.* **36,** 927 (1991).
6. H. Ehrenberg, H. Weitzel, H. Paulus, M. Wiesmann, G. Wltschek, M. Geselle, and H. Fuess, *J. Phys. Chem. Sol.* **58,** 153 (1997).
7. L. Merrill and W. A. Bassett, *Rev. Sci. Instrum.* **45,** 290 (1974).
8. H. Ahsbahs, *Rev. Sci. Instrum.* **55,** 263 (1984).
9. H. Ahsbahs, R. Dorwarth, K. Hölzer, and W. F. Kuhs, *Z. Kristallogr. Suppl 7*, 3 (1993).
10. J. D. Barnet, S. G. Block, and L. Piermarinie, *Rev. Sci. Instrum.* **44,** 1 (1973).
11. L. W. Finger and H. King, *Am. Mineral.* **63,** 337 (1978).

12. G. M. Sheldrick, "SHELXS-86: Program System for the Solution of Crystal Structures." University of Göttingen, 1986.
13. G. M. Sheldrick, "SHELXL-86: Program for Crystal Structure Determination." University of Göttingen, 1993.
14. O. Shimomura, S. Yamaoka, T. Yagi, M. Wakatsuki, K. Tsuji, H. Kawamura, N. Hamaya, O. Fukunaga, K. Aoki, and S. Akimoto, "Solid State Physics Under Pressure," p. 351. Terra Scientific, Tokyo, 1985.
15. T. J. B. Holland and S. A. T. Redfern, *Mineral. Mag.* **61,** 65 (1995).
16. F. D. Murnaghan, "Finite Deformation of an Elastic Solid." Wiley, New York, 1951.
17. R. J. Hill and C. J. Howard, Australian Atomic Energy Commission Report No. 112, 1986.
18. L. Kihlborg and E. Gebert, *Acta Crystallogr.* **B27,** 1020 (1970).
19. A. W. Sleight and B. L. Chamberland, *Inorg. Chem.* **7,** 1672 (1968).